Chapter 8

Spectromicroscopic characterization of organic layers

PhotoElectron Spectroscopy (PES) is a widely and successfully used method to study the stoichiometry, the chemical composition and bonding, and the electronic states [87, 88, 89]. In particular, the method is suited to investigate the growth and bonding properties of hybrid systems such as organic layers adsorbed on metal substrate surfaces. Here, the interface bonding is of special interest for multiple reasons. From the practical point of view the bonding at the interface and the potential barriers formed at the interface limit the charge transport and therefore the performance of organo-metallic electronic devices. Concerning the fundamental aspects, many of the properties of organic layers and interfaces are poorly — or even not at all — understood.

In many cases, PES alone, i.e. without lateral resolution, is not sufficient for a deep understanding of the interface bonding. Typically, PES integrates over large areas of ~ 1 mm^2 on the sample surface and therefore the *local* spectral information is lost. Furthermore the spectroscopic method is very often, due to experimental reasons, relegated to control the growth of films prepared in dedicated chambers. Then the sample is spectroscopically analyzed *post-growth* in a neighboring vacuum-connected chamber. If the vacuum is not preserved in the transfer process then the measurement procedure is known as *ex-situ*. Both difficulties can be overcome by means of spectro-microscopy, where *in-situ* and local spectroscopic information is accessible. The combination of

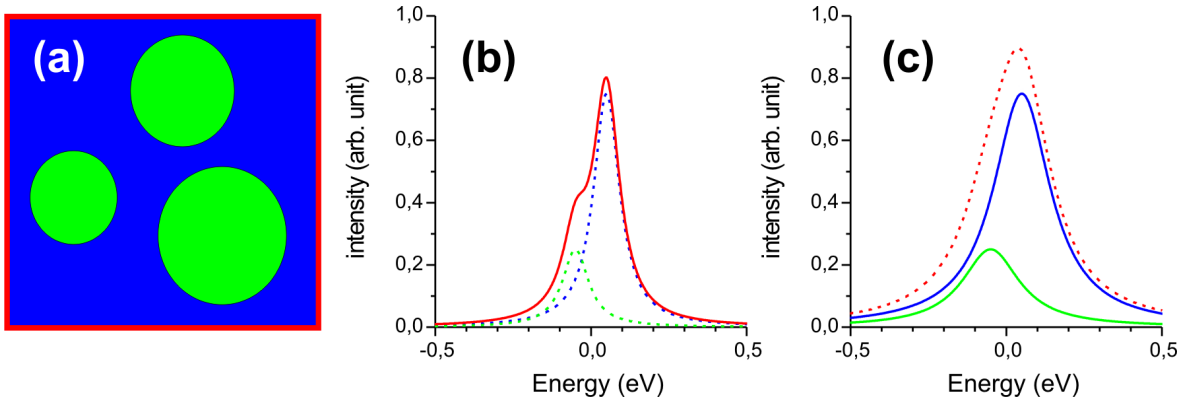

Figure 8.1: Comparison between Spectro-microscopy and Spectroscopy. (a) Microscopic view of the surface composition (ratio 3:1 of blue:green regions), (b) shows the overall spectra (red) and the fit with two peaks (dashed green and blue lines) with $w_L = 0.1$ eV and $w_G = 0.02$ eV, (c) shows the micro-spectra from the green and blue area with $w_G = 0.2$ eV.

spectroscopy with microscopy bears, however, a setback by the fact that it has a lower spectral resolution if compared to that of a conventional spectrometer.

How the advantages of the spectro-microscopic method compensate for this loss in energetic resolution can be understood in the following example (figure 8.1). Consider a surface composed of two elements with a stoichiometric ratio of 3:1, and core level peaks separated by 0.1 eV and with a Lorentzian width of 0.1 eV each. Let us assume that the spectro-microscope has an energy resolution of 0.2 eV and the spectrometer of 0.02 eV. This would result in a considerable broadening of peaks for the microscope (figure 8.1.c), whereas a spectrometer measures the sum of the peaks, nearly not affected by instrumental broadening (figure 8.1.b). Nevertheless, in the case of the averaging spectrometer the individual peaks can only be distinguished by peak fitting the data. In contrast to this, a spectro-microscope delivers directly the individual spectra, as far as the A and B domains can be laterally resolved. Therefore, the intensity ratio and peak separation can be measured without any fitting.

In the following sections two spectro-microscopic techniques applied to the investigation of the growth of PTCDA on Ag(1 1 1) are presented. In the first example we take advantage of the real-time spectroscopic measurement during growth from a small sampled area of $\sim$ 40 μm^2. The *in-situ* real-time dynamic observation of the evolution of the photoemission spectrum during growth allows to monitor eventual

intermediate or metastable phases that would otherwise be missed with conventional *ex-situ* or *post-growth* spectroscopy. Furthermore, the experimental conditions (temperature, evaporation rate, pressure, etc...) are the same throughout the experiment and no energy re-calibration is necessary. Also the intensity of the peaks can be directly compared without thickness normalization. However, one has to make sure that the irradiation does not significantly influence the process under consideration.

The second section is dedicated to the combination of spectroscopy with microscopy. We study the *in-situ* prepared thin PTCDA film on Ag(1 1 1) with laterally-resolved NEXAFS spectroscopy. The benefit of such a comprehensive characterization lies in the investigation of the molecular orientation in regions covered by 2 or 3 layers of PTCDA as compared to PTCDA crystallites *in one single measurement*. Furthermore it is possible to differentiate the spectroscopic properties between different 3D-islands. This will be specifically addressed in the circular dichroism section, dealing with the chirality of individual crystallites. The spectroscopic properties of similar individual organic crystallites have also been recently investigated in the work of *Groh* [26].

8.1 *In-situ*-PES during growth

Most PES methods cannot directly observe the film during growth, and hence the spectroscopy carried-out on the grown film *ex-situ*. The film properties are therefore investigated by indirect measurements and strongly relying on delicate parameters such as the calibration of the evaporation rate. The eventual formation of intermediate metastable or transition phases may only be revealed by *in-situ* real-time spectroscopy. In the following we opted for monitoring *at once* a whole spectrum of about 15 eV width while growing a thin film of PTCDA on Ag(1 1 1). Alternatively we could have used energy filtered XPEEM to image the photoemission from a small kinetic energy window centered on a relevant core level peak. Unfortunately, in our case, the intensity from the C 1s or O 1s would have been too low rendering the laterally resolved imaging useless. Furthermore, the most significant chemical shifts occur from the C 1s and O 1s core levels. Of the two we have opted in this case for the C1s spectra. Thus we have measured the evolution of the C 1s core-level photoemission spectra during the growth of PTCDA on Ag(1 1 1). The results are shown in figure 8.2. An overview of

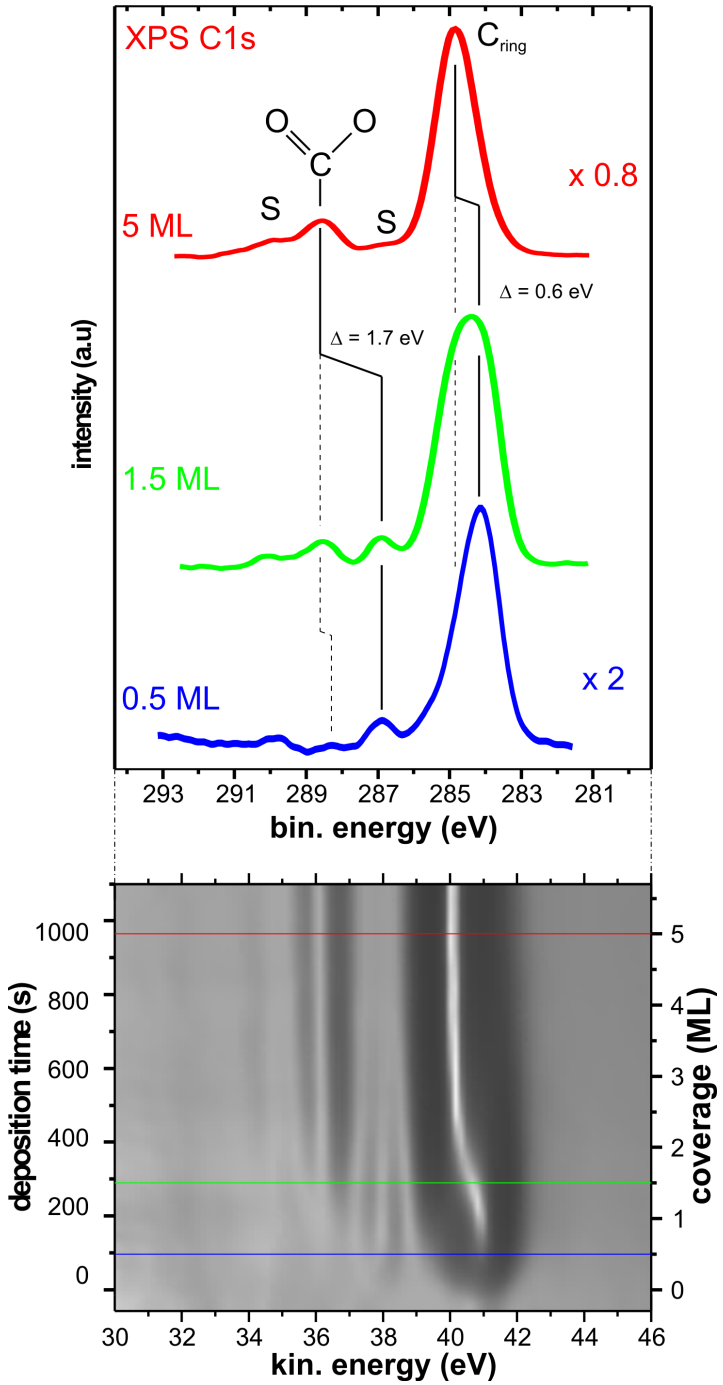

Figure 8.2: In-situ PES during growth. Top: three carbon 1s spectra of different coverages (in nominal monolayers) of PTCDA on Ag(1 1 1). The main peaks and shake-up satellite peaks ('S') are indicated. Bottom: time evolution of the spectrum (top view of a surface in 3-dimensions). For details, see text.

Table 8.1: Parameters used for the results shown in figure 8.2

Sample Ag(1 1 1)	T = 250 K
Microscope	Sample potential = 34.5 eV
	Kinetic energy range = 30 — 46 eV
	Binding energy range = $\sim$ 295 — 279 eV
	Probed area = $\sim$ 38 μm^2
	Acquisition time = 10 sec
	Acquisition rate = 1 image/12 sec
	Images per layer = 16
Analyzer	contrast aperture d_c = 70 μm
	Magnification M_{Tr} of transfer optics = 8
	Entrance slit (d_c/M_{Tr}) = 8.8 μm
	Entrance energy width ($d_c/M_{\mathrm{Tr}}/35\frac{\mu m}{eV}$) = 0.25 eV
	Field aperture d_a = 1000 μm
	Selected area diameter $d_a/M_{\mathrm{Tr}}/M_{\mathrm{Obj}}$ = 7 μm
Evaporator	Deposition rate = 192 sec/ML
Beam line	$h\nu$ = 330 eV
	Exit slit = 100 μm
	c_{ff} = 10 μm

the parameters used to perform the measurements is given in table 8.1.

The lower part of figure 8.2 there is a 2d-plot of the intensity as a function of the kinetic or binding energy on the abscissa and deposition time or coverage on the ordinate. In the upper part of the figure there are three spectra, extracted from the 2d-intensity plot, taken at coverages of 5, 1.5 and 0.5 nominal layers (top to bottom) as indicated by the red, green, and blue horizontal lines, respectively. The determination of the thickness has been done by meticulous evaporator calibration.

Two main features are visible in the 2d-intensity plot that shift towards higher binding energies starting at the closure of the first monolayer and last until the closure of the second one. The main asymmetric peak is observed in the multilayers spectrum at about 285 eV and the smaller peak at about 288.5 eV. The main peak is attributed

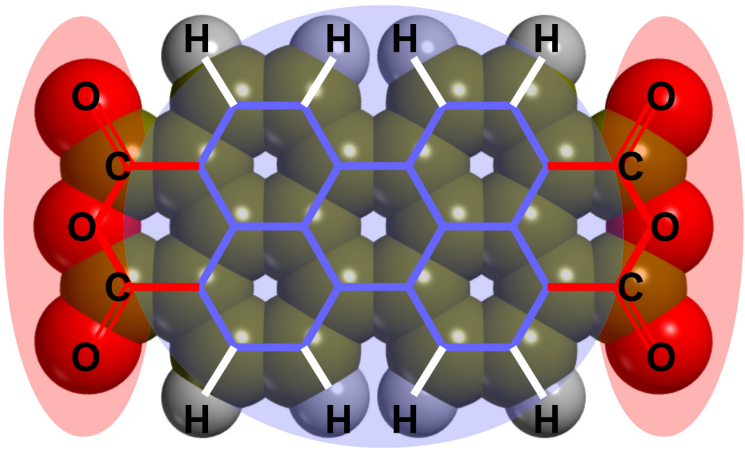

Figure 8.3: Schematic view of the PTCDA molecule with the regions highlighted from which the two main peaks of figure 8.2 originate. The larger peak in the multilayer spectrum of figure 8.2 is associated with the C1s emission from the aromatic perylene core (blue region). The smaller peak is related to the carboxylic carbon species (red region).

to the photoemission from the C 1s levels of the carbon atoms in the aromatic perylene core and consists of at least four different contributions that are not resolved. The smaller peak at 288.5 eV originates from the C1s photoemission of the carboxylic carbon atoms of the anhydride group. Figure 8.3 schematically highlights the aromatic perylene core with a blue shading and the carboxylic carbon region with a red shading. These peak assignments have been investigated in detail in Ref. [90, 91, 47]. The large difference in the number of atoms belonging to each group, 20 for the perylene core and 4 for the carboxylic region, is reflected in the large difference in the areas of the two peaks[1]. A possible approach to understand the peak assignment is to simply consider the higher electronegativity of oxygen that results in an ionic contribution to the carbon–oxygen bond. This causes a slight charge transfer which causes a higher binding energy in the initial state and in addition leaves the core hole final state less screened. In the multilayer spectrum two other small features are visible and have been labelled with an 'S', they are identified as shake-up satellites. These final state effects have been investigated in detail by *Jung et al.* [90] and are mainly attributed

[1]For the calculation of the correct stoichiometry the satellite peak areas must be included. This has been shown to be the case by *Zou et al.* [47].

to intramolecular $\pi \rightarrow \pi^*$ transitions. They furthermore show that a charge transfer occurs in the core ionized molecule by excitation of an electronic charge from the aromatic part, acting as a donor, to the accepting anhydride group.

The comparison between the monolayer (blue curve at the bottom) and the multilayer (red curve at the top) curve shows a shift in the position of the two main peaks towards higher binding energies of 0.6 and 1.7 eV for the peaks previously attributed to the perylene core and the anhydride group, respectively. The strong change in binding energy is a clear indication that the molecule in the monolayer strongly interacts with the substrate, i.e. is chemisorbed. The increase of both peaks in binding energy is an indication of a less effective screening of the core hole final state by the image charge or by charge transfer[2] screening. The screening is clearly not as effective in the multilayer probably due to a lower effective delocalization of the electrons. We furthermore notice that the shift of the carboxylic carbon 1s peak is stronger than in the case of the perylene core. This must originate from a different image charge or higher charge transfer screening effectiveness of the carboxylic carbon and can be used to speculate on the higher bonding efficiency of the carboxylic functional group.

The intermediate spectra of 1.5 nominal layers of PTCDA/Ag(1 1 1) shows both features of the multilayer and of the monolayer. This is a strong indication that the bonding transition from one layer to multilayer, which determines the peak positions and is due to the bonding and the charge transfer and screening efficiency, occurs already at the second layer. This is an indication that the second layer, from a spectroscopic point of view, exhibits bonding properties that are similar or identical to those of the multilayer.

8.2 NEXAFS investigations of PTCDA on Ag(1 1 1)

NEXAFS has proven itself to be an ideal technique to determine the molecular orientation, the interface bonding and the electronic properties especially for the unoccupied

[2]In the first layer of PTCDA on Ag(1 1 1) there is a charge transfer from the metal substrate to the LUMO of the molecule. This will be shown in the following section with NEXAFS.

states of adsorbates on solid surfaces [62]. The particular case of aromatic molecules adsorbed on metals has attracted a strong interest due to the present practical applications of organic semi-conductive devices, and many more applications are looked at for the future. Interestingly little is known about the details of these molecular solids and the interfacing to metal substrates. Among many others, mainly two large organic aromatic molecules, PTCDA and NTCDA, have received much attention by the scientific community dedicated to the understanding of their fundamental properties. For instance in the case of NTCDA, with a sufficiently high photon energy resolution from undulator beamlines at 3rd generation synchrotron sources, the coupling of the NEXAFS transition to vibronic excitations has been resolved [92] allowing for a very detailed analysis of the electronic and chemical state. NEXAFS, as a leading technique for the investigations of unoccupied electronic states can also reveal insight into the *local* bond properties (intermolecular interactions) and is hence part of this work. In the following we will not focus on the high photon energy resolution, but on the information obtainable from the laterally resolved contributions of NEXAFS. We have already discussed the image contrast formation in section 5.2 on page 51 and we will now report on the scientific results from the investigations of PTCDA on the Ag(1 1 1) surface.

Figure 8.4 shows in the far right column NEXAFS spectra of the C1s $\rightarrow \pi^*$ transition for four different polarizations of the incoming light and in each figure three spectra are taken from different selected sample regions. The polarization and geometry of the electrical field polarization vector $\overrightarrow{\mathbf{E}}$ with respect to the sample is schematically depicted in the first column. Notice that in the first two rows the polarization is linear and in the last two circular. The shown XPEEM images have been extracted from a stack of 70 images, measured in the photon energy range from 283 to 290 eV (ΔE = 0.1 eV). The intent of the figure is to present a data set with the four polarizations. To avoid beam damage, we have therefore measured in a small energy range (if compared to NEXAFS spectra of similar molecules in the literature).

The PTCDA NEXAFS spectrum is reasonably complicated and has been treated in detail elsewhere in the literature [91]. Some simple details of the spectra will also be exploited here, especially regarding the main features and their physical origin within the molecule. Of the displayed images, the ones at 283.0 eV have been taken before the

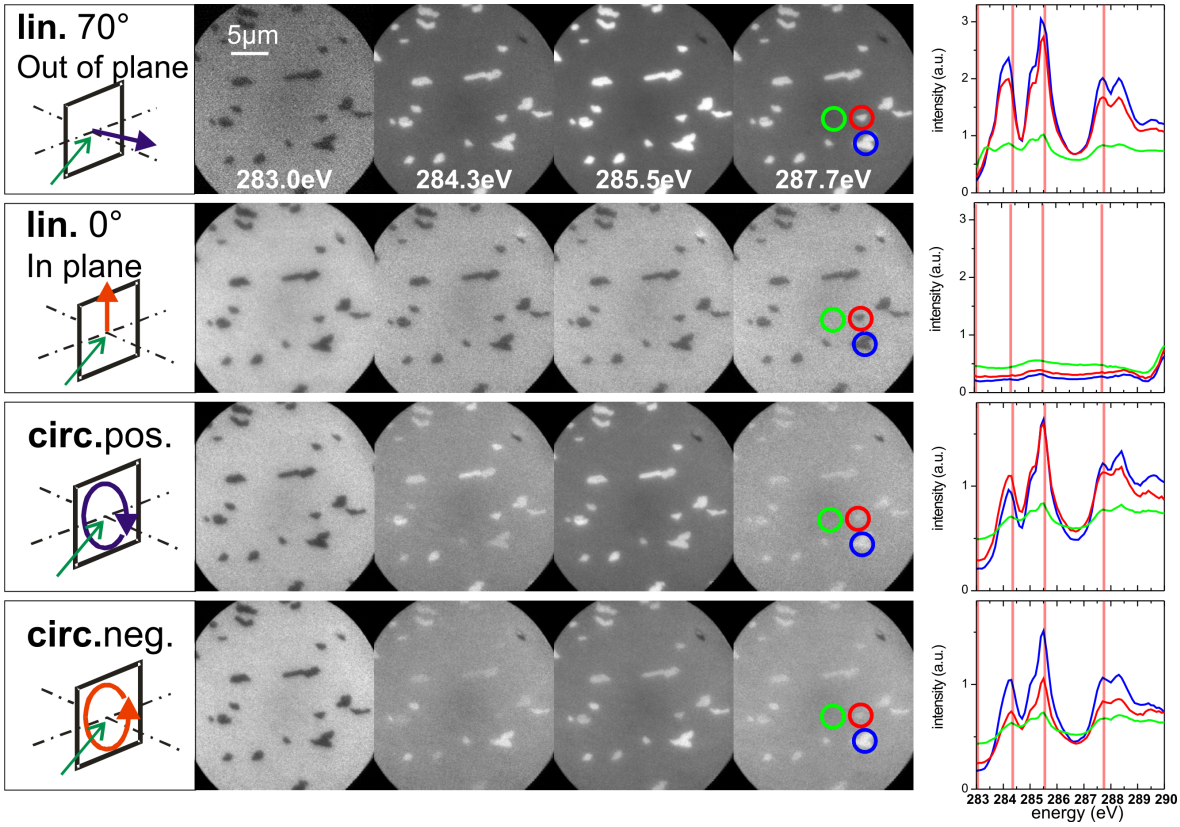

Figure 8.4: Laterally resolved NEXAFS scans of 5 nominal PTCDA layers on the Ag(1 1 1) surface at 366 K. Every row shows, from left to right, (1) the light polarization with respect to the surface, (2) four XPEEM images taken at photon energies of 283.0 eV, 284.3 eV, 285.5 eV and 287.7 eV, (3) NEXAFS spectra generated from the areas highlighted by the colored circles (green = bilayer, red and blue = 3D-islands). From the top to the bottom column the light polarization is changed.

start of the resonance, in this case and the contrast is simply due to the attenuation of the electrons emitted in the substrate by the PTCDA film as discussed in section 5.2 on page 51. The following three images at 284.3, 285.5, and 287.7 eV are representative of the main three C1s $\rightarrow \pi^*$ transitions appearing in the spectra. The first two peaks, at about 284 and 285-286 eV, are due to transitions from the 1s level of the carbon atoms located in the perylene backbone to the first unoccupied molecular orbitals (LUMO, LUMO+1 and LUMO+3). The *main* contribution to the C1s $\rightarrow \pi^*$ transition in the third peak at about 288 eV is due to the carbon atoms in the anhydride group. The discussion is now divided into two main blocks, in which the linear and circular dichroism are treated separately.

8.2.1 Linear dichroism

In the following the orientation of the molecules in the grown film will be discussed by comparing the differences in the spectra with respect to different polarizations of the incident light. Due to simple geometric considerations one can evaluate relatively easily an average orientation from the NEXAFS spectra. Details of the analysis concept are summarized in the the book of *Stöhr* [62]. The exploitable information of the microscopic approach is then compared to conventional, i.e. laterally averaging, NEXAFS measurements. As the last aspect the normalization of the NEXAFS spectra is discussed, placing again emphasis on the microscopic point of view of the normalization procedure and its advantageous applications to the investigation of PTCDA bilayers.

Figure 8.5 shows six spectra taken in the energy region, from 282 to 294 eV that have been normalized to same intensity before and after the π^* resonance, for better comparison. The green spectra have been taken from the two layer thick region, the blue from a three layer region and the red from a 3D-crystallite. The linearly polarized light was either with the $\overrightarrow{\mathbf{E}}$-vector forming an angle of 70° or 0° with the surface plane. The lack of resonances for the spectra with $\overrightarrow{\mathbf{E}}$ in the surface plane (i.e. 0°) implies that the molecules are lying flat on the surface in all sample regions. That means that the perylene core, and its π^* orbitals, are parallel to the surface. The interesting non necessarily expected aspect is that the molecules are lying flat *everywhere* on the surface.

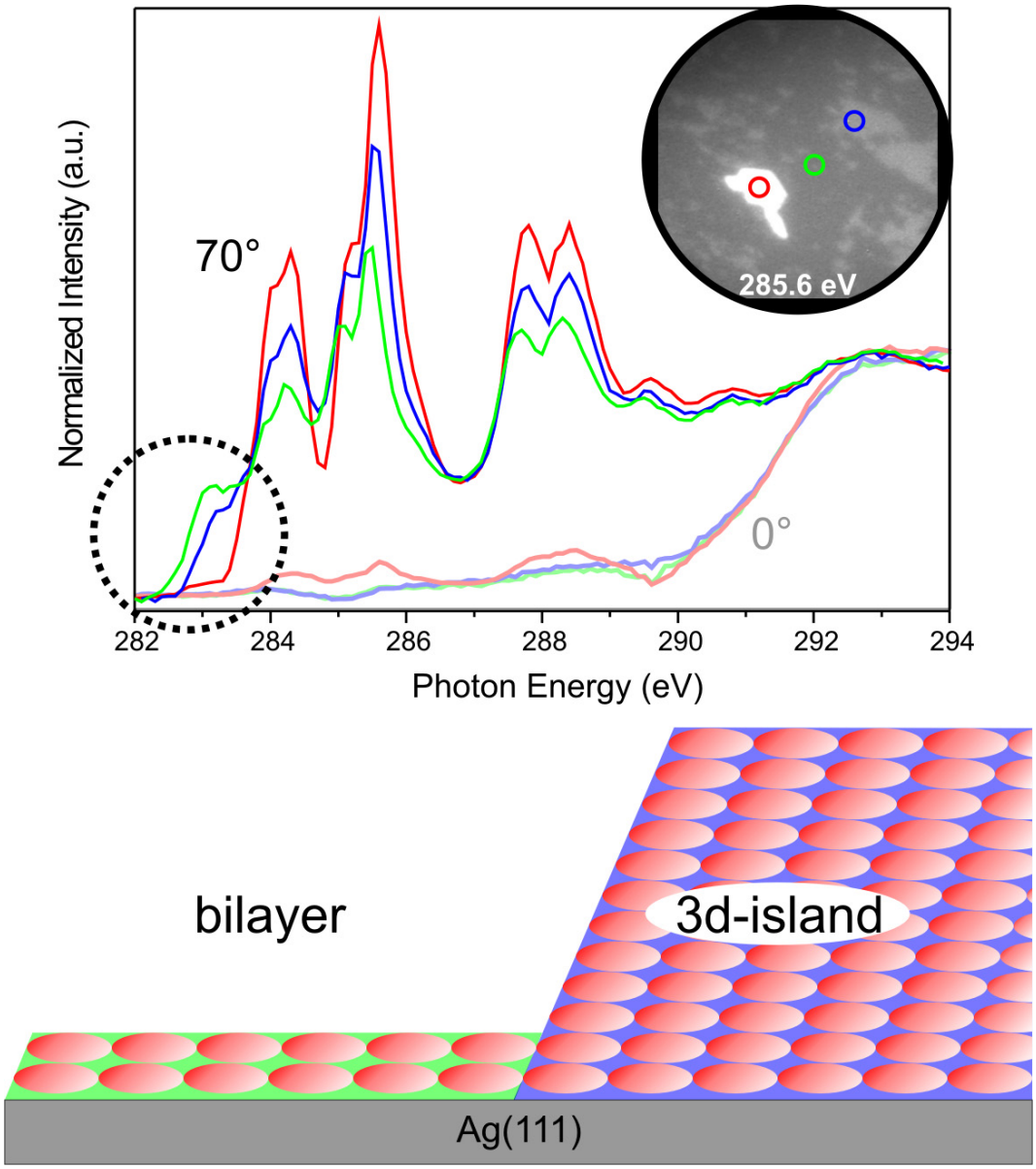

Figure 8.5: Molecular orientation in NEXAFS. Comparison of the NEXAFS spectra for two polarizations (0˚ and 70˚) and three sample regions (shown in the inset) (top) and relative molecular orientation (bottom) for a PTCDA bilayer (a) and 3D-island (b) on the Ag(1 1 1) surface.

The next important advantage of using a spectro-microscopic method is related to the normalization procedures used in NEXAFS. The data presented in figure 8.5 has been normalized by division with the photon flux curve which, in our case like in most of the investigations of organic thin films on metal substrates, is obtained from running a NEXAFS scan on the clean substrate without adsorbates (see [62]) assuming that the substrate has no spectroscopic structure in this energy range, which is the case for the Ag and Au surfaces. Furthermore the energetic positions of the intensity minima in the flux curve of the beamline (two strong features due to carbon contamination on the x-ray optics) vary with time [93] and depend on polarization. Additionally an incorrect energy scale calibration can lead to the appearance of artifacts in the NEXAFS spectra [94]. This off-line normalization method may also suffer from slight miscalibration of the beamline x-ray optics. It becomes clear that the normalization of spectra can be rather challenging for thin films of two layers or less where the signal from the adsorbate is extremely low compared to the background, resulting in spectra with high noise. The advantage in using a microscopic method is that the energy calibration can be done on a region of the sample with high intensity, e.g. from a 3D-islands, and the same normalization can be applied to the thinner layers within the image without further re-calibration or corrections. This normalization allows us to reproduce features arising from thin films with the confidence of not creating artifacts.

Our goal in the following is thus to extract information from the thin film, a 2 ML and a 3 ML region, and to relate this to the interface properties. Investigating a 2 ML and a 3 ML film has also the advantage that the interface is *buried* under the second layer, thus reproducing more realistically the environment of the multilayered PTCDA/Ag(1 1 1) interface. However, the spectrum of the buried interface has to be extracted and for this purpose the simplest approach would be to consider the second layer as having the same NEXAFS features as the multilayer. This is however a bad compromise because the multilayer is a superposition of the spectra from many layers, one over the other. Thus the emission from the deepest layer is exponentially attenuated, and the absolute intensity contribution of one single layer is hardly extractable. In our analysis we have therefore restricted ourselves to the part of the spectra before the on-set of the multilayer π^* resonance (C1s $\rightarrow$ LUMO). In the bottom left of the graph in figure 8.5 a small circle marks the on-set of the NEXAFS resonance. Notice

that the peak observable in the 2 ML spectrum (green curve) is slightly reduced in the 3 ML spectrum (blue curve) and nearly vanishes in the 3D-islands spectrum (red curve). The origin of this feature, which lies below the known LUMO resonance of the 3D-island spectrum (at about 284 eV), is therefore assigned to the interface PTCDA layer.

This finding has been already extensively investigated with Electron Energy Loss Spectroscopy (EELS) [48] and with PES and NEXAFS [47], and is explained as follows. In the multilayer, the LUMO is located above the Fermi level, as it would be expected, and it is separated from the HOMO in the molecular solid by 2.5-3 eV [48]. Upon adsorption, the LUMO of the interface layer is hybridized with the 4s-levels of the Ag(1 1 1) forming a partially filled band that crosses the Fermi level. The complete energy level scheme has already been shown in figure 3.3 on page 28. In the 3D-island NEXAFS spectrum the LUMO orbital, from which the peak at the lowest photon energy is formed, is just above the Fermi level and is completely empty, just as one would expect. When adsorbed, the NEXAFS intensity from the LUMO is drastically reduced, lowered in energy and cut by the Fermi level[3]. The lowering in intensity is an indication that at the interface the LUMO is almost completely filled and energy levels are available just above the Fermi level. This corroborates the involvement of the LUMO in the formation of the interface bond and the charge transfer from the metal to the LUMO at the interface responsible for the (slight) increase of the work function (which is partially compensated by a charge back-donation, as mentioned in 5.1.1).

8.2.2 Circular dichroism

Optical activity is referred to the rotation of linearly polarized light upon transmission through a medium and has been found experimentally for the first time more than 200 years ago for crystalline quartz. Fresnel proposed thereafter that optical activity is related to different absorption for left and right circularly polarized light, i.e. Circular Dichroism (CD). The extension of optical activity to the x-ray energetic region has been done only in recent years. X-ray absorption CD has been observed for magnetic surfaces (XMCD = X-ray Magnetic Circular Dichroism) [95, 96] and only very recently

[3]The position of the Fermi level has not been determined experimentally, but is adapted from [47].

for molecular [97] and ionic crystals [98] (XNCD = X-ray Natural Circular Dichroism). Whereas the first method is widely spread when combined with PEEM [99, 100], we have not found any XNCD effects observed in PEEM.

The *dipole approximation* assumes a constant electrical field over the atomic volume in the propagation direction of the x-ray light. This results in a truncated expansion of the exponential function to the first term ($e^{i\vec{k}\cdot\vec{r}} \approx 1$). Such approximation fails when trying to account for CD which arises from higher terms of the expansion. The approach is therefore to include the second term resulting in the truncated expansion $e^{i\vec{k}\cdot\vec{r}} \approx 1 + i\vec{k}\cdot\vec{r}$. The main difference results from the fact that the x-ray absorption process becomes wavevector-dependent, and the electromagnetic field cannot be assumed to be uniform over the atomic volume. The nature of the incident light can be considered to have a chirality that arises from the rotation of the electrical field around the propagation axis. This type of chirality is defined as *spatial chirality*. The different absorption cross section for left and right circularly polarized light is therefore described as a different interaction between the chirality of the crystal with the (spatial) chirality of the light.

While electric dipole transitions (i.e. according to the dipole approximation) are associated with an electron transfer along a linear path, e.g. from an s- to a p-orbital, the quadrupole transition does not occur along *one* direction because the quadrupole moment is a tensor. An example of quadrupole transitions is that from an s- to a d_{yz}-state.

We have deposited PTCDA on the Ag(1 1 1) surface and measured the differential circular dichroism signal. Figure 8.6 shows a larger set of a sequence of images that were already presented in figure 8.4 with more details. The graph shows the differential CD signal as a function of photon energy for three different regions of the surface identified by three colored circles. In the image in the bottom right the dichroic crystallites are distinguished.

The two spectra obtained are used as fingerprints for the identification of the *enantiomeric* crystallites (shown in the bottom right of figure 8.6). We notice that no differential dichroism spectrum would have resulted from an averaging method, because the two types of crystallites exhibit the opposite CD behavior and the two would cancel out each other. Once again, the clear advantage of spectro-microscopy is the

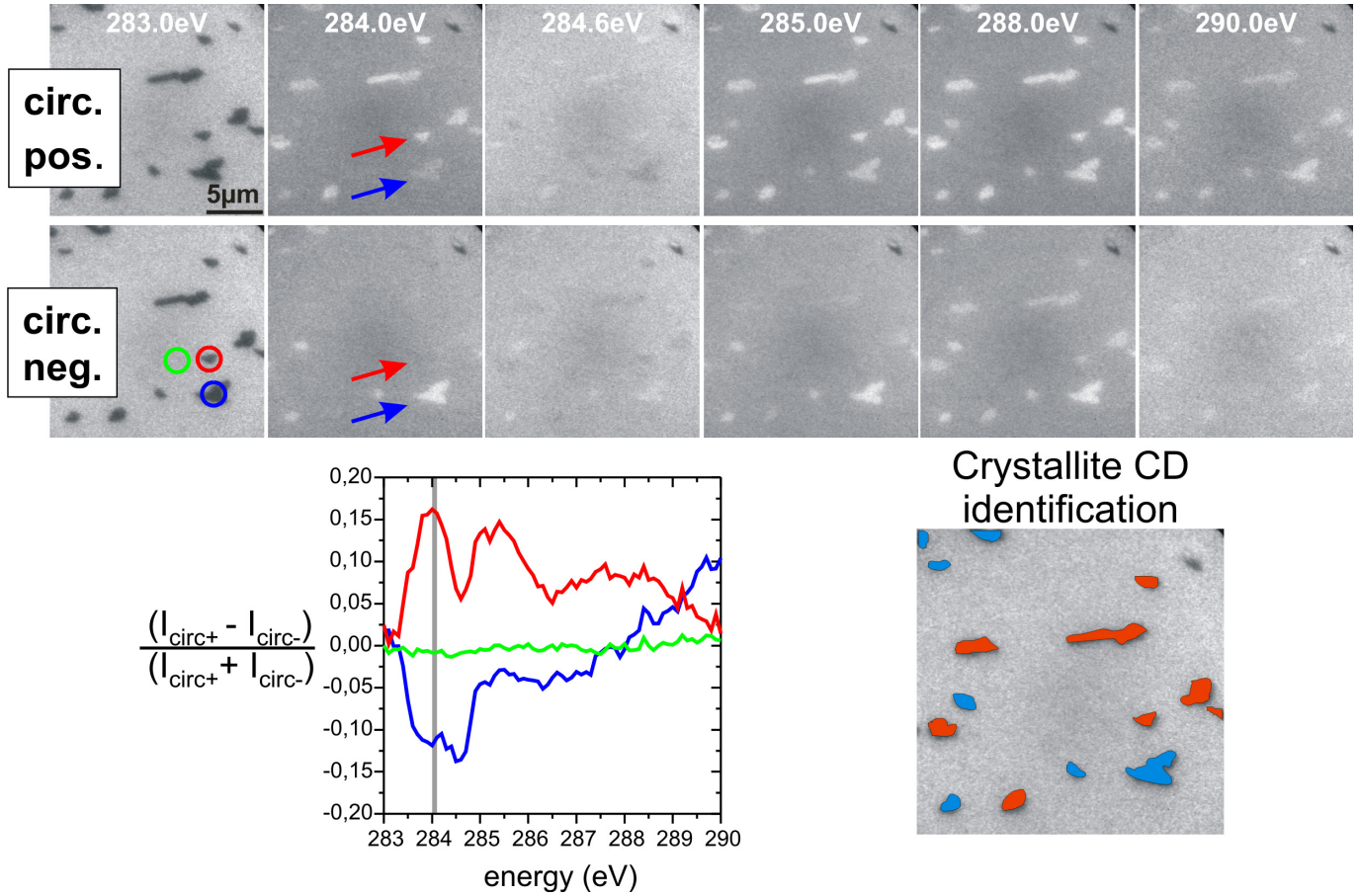

Figure 8.6: Circular Dichroism-NEXAFS: The images in the first two rows are extracted from a stack of 70 XPEEM images that compose the full NEXAFS spectrum. The two rows differ in circular polarization (positive and negative helicity). The bottom graph shows the dichroic signal for three different areas on the sample. The color labelled image in the bottom right identifies the crystallites with the two types of the CD.

characterization of properties on inhomogeneous surfaces which would pass unobserved in averaging methods.

These measurements show an extremely strong natural CD and are very convincing for the following reasons. In the images taken at 284.0 eV in figure 8.6, two arrows, red and blue, point at two crystallites with dichroic contrast inversion. In the spectrum in the lower part of the figure a vertical line at 284.0 eV highlights the position of this contrast inversion. This is where the highest contrast, i.e. circular dichroism, is obtained between the red and blue labelled crystallites. The presence of two crystallites within the same image less that 2 μm apart that exhibit opposite dichroic properties excludes that the findings are experimental artifacts generated by elliptically polarized light. Even inhomogeneities, such as a progressive transition from a dominant horizontal to vertical electrical field component in the elliptically polarized light can be excluded because the distribution of the crystallites on the surface appears random. Furthermore, even though the signal from the bilayer is weak, it clearly shows no dichroic signal (green spectrum) thus also providing the absence of x-ray beam inhomogeneities.

To explain the CD spectra, the geometrical arrangement of the molecules in the crystallites has to be considered. Due to the combination of the structure in the (1 0 2) planes of crystalline PTCDA, often called herring bone structure, with the intramolecular charge displacement (due to the higher electronegativity of the anhydride groups), the molecules can exhibit a quadrupole moment. The CD arises from an interference of electric dipole and electric quadrupole transitions. The presence inside the molecule of a quadrupole moment could therefore be at the origin of the experimentally observed CD. However, preliminary calculations by *Stöhr et al.* [101] have shown that the expected signal for our system should be lower than 1 %. In our measurements, the highest signal observed is as large as 15 %.

8.3 Spectro-microscopy: how far can it go?

The spectroscopic applications of a microscope have been explored using PTCDA thin films on the Ag(1 1 1) surface. The methods applied revealed a wide-ranging set of information, all from the same instrument, that has shed some light upon unanswered questions. For instance, due to the continuous monitoring of the XPS data we can

exclude the presence of metastable layers exhibiting a characteristic spectrum. This could be reasonable during the growth process and such an effect would be missed by a static method that studies the film only at distinct thicknesses. Furthermore the surprisingly high quality of the PES measurements, which could be compared with those from dedicated instruments (hemispherical analyzers), is combined with one of the strongest advantages of the instrument: the *real-time* PES observation of the growth. The summarization of the benefits of this measurement are that

- the presence of intermediate phases with a characteristic spectrum can be excluded,
- the growth parameters (temperature, evaporation rate, pressure, etc...) are constant,
- the peak positions can be directly compared excluding artifacts arising from the energy calibration and
- the peak areas can be directly compared without thickness normalization.

When these measurements where performed the resolution of the energy analyzer had not yet been optimized. However, peak shifts of 0.7 eV are easily resolved. Often the differences observed in surface core level shifts or more simply in chemical composition can only be observed with an improved instrumental energy resolution. This is already the case, because the readily available energy resolution is better than 180 meV.

The next interesting aspect regards the laterally resolved NEXAFS measurements. Again most of the details of conventional high-resolution NEXAFS spectroscopy have been successfully reproduced, but we could gain access to distinct surface regions (bilayer and 3D-islands) and directly compare the spectra. Access to such information allows for a comprehensive characterization of the unoccupied orbitals (the LUMO) at the interface and in the molecular crystal.

The pressing question now is "What can still be done?". The obvious answer is the combination of spectroscopic information, such as that described in section 8.1, with the advantages of the lateral resolution already mentioned in section 8.2. An example is shown in figure 8.7. Here only images at the photon energy of $h\nu = 285.1$ eV are shown, but the actual data set is comprised of a continuous cycle of images taken

Figure 8.7: *in-situ* NEXAFS-PEEM: Set of images taken during growth with $h\nu = 285.1$ eV. The images have been made at 10 different energies within the NEXAFS C 1s $\rightarrow \pi^*$ spectrum at the energy positions of a significant transition *during growth* (see text for details). After each scan of 10 images, a new one started without interruption of the deposition.

at ten significant photon energies (before resonance, on the π^*-perylene core resonance, on the π^*-anhydride and on the σ^* orbitals) *during* the growth of the thin film. The resulting method is a "fast-scan" NEXAFS-microscopy *during* growth. In such a measurement dynamic information of the real-time evolution of the thin film during growth can be probed, but with limited energetic resolution. The acquisition rate of such measurements is mainly determined by the speed of the mechanics of the beamline monochromator and of the undulator and has been optimized regarding the signal to noise ratio and the beam damage rate of our organic film. At the chosen field of view the latter is the dominating factor, so that the density of measured energy points and hence the energy resolution had to be reduced. However, we believe that such measurement methods should be further exploited, specially for the real-time dynamic spectro-microscopic investigations of the growth of *non-radiation sensitive* thin films.